Stability versus Meta-stability in a Skin Microbiome Model

Eléa Thibault Greugny, Georgios N Stamatas, François Fages

Stability versus Meta-stability in a Skin Microbiome Model

Eléa Thibault Greugny[1,2], Georgios N. Stamatas[1], and François Fages[2]

[1] Johnson & Johnson Santé Beauté France, Issy-les-Moulineaux, France
[2] Inria Saclay, Lifeware Team, Palaiseau, France

Abstract. The skin microbiome plays an important role in the maintenance of a healthy skin. It is an ecosystem, composed of several species, competing for resources and interacting with the skin cells. Imbalance in the cutaneous microbiome, also called dysbiosis, has been correlated with several skin conditions, including acne and atopic dermatitis. Generally, dysbiosis is linked to colonization of the skin by a population of opportunistic pathogenic bacteria (for example *C. acnes* in acne or *S. aureus* in atopic dermatitis). Treatments consisting in non-specific elimination of cutaneous microflora have shown conflicting results. It is therefore necessary to understand the factors influencing shifts of the skin microbiome composition. In this work, we introduce a mathematical model based on ordinary differential equations, with 2 types of bacteria populations (skin commensals and opportunistic pathogens) to study the mechanisms driving the dominance of one population over the other. By using published experimental data, assumed to correspond to the observation of stable states in our model, we derive constraints that allow us to reduce the number of parameters of the model from 13 to 5. Interestingly, a meta-stable state settled at around 2 days following the introduction of bacteria in the model, is followed by a reversed stable state after 300 hours. On the time scale of the experiments, we show that certain changes of the environment, like the elevation of skin surface pH, create favorable conditions for the emergence and colonization of the skin by the opportunistic pathogen population. Such predictions help identifying potential therapeutic targets for the treatment of skin conditions involving dysbiosis of the microbiome, and question the importance of meta-stable states in mathematical models of biological processes.

Keywords: skin microbiome · atopic dermatitis · ODE model · steady-state reasoning · parameter relations · quasi-stability · meta-stability.

1 Introduction

Located at the interface between the organism and the surrounding environment, the skin constitutes the first line of defense against external threats, including irritants and pathogens. In order to control potential colonization of the skin surface by pathogens, the epidermal cells, called keratinocytes, produce antimicrobial peptides (AMPs) [26]. The physiologically acidic skin surface pH also

contributes to control the growth of bacterial populations [27, 17]. Another contributor to the defense against pathogen colonization are commensal bacteria in the community of microorganisms living on the skin, commonly referred to as the skin microbiome. Over the past decade, several studies have highlighted the key role played by such commensal bacterial species defending against invading pathogens, as well as their contribution to the regulation of the immune system [19, 5, 18, 15, 1, 2].

Alterations in the composition of the skin microbiome resulting in a dominance by a pathogenic species, also called dysbiosis, have been associated with skin conditions such as acne or atopic dermatitis (AD) [20, 16]. In the case of AD, the patient skin is often colonized by *Staphylococcus aureus* (*S. aureus*), especially on the lesions [16]. Treatment strategies targeting non-specific elimination of cutaneous microflora, such as bleach baths, have shown conflicting results regarding their capacity to reduce the disease severity [4]. On the other hand, treatments involving introduction of commensal species, like *Staphylococcus hominis* [24] on the skin surface appear promising. Accordingly, the interactions between the commensal populations, pathogens and skin cells seem at the heart of maintaining microbiome balance. There is therefore a necessity to investigate further those interactions and the drivers of dominance of one population over others. Unfortunately, it is challenging to perform *in vitro* experiments involving more than one or two different species, even more so on skin explants or skin equivalents.

Mathematical models of population dynamics have been developed and used for more that 200 years [21]. Here, we introduce a model based on ordinary differential equations (ODEs), describing the interactions of a population of commensal species with one of opportunistic pathogens and the skin cells. We study the factors influencing the dominance of one population over the other on a microbiologically relevant timescale of a couple of days corresponding to biological experimental data. More specifically, we identify constraining relationships on the parameter values, based on published experimental data [23, 14], corresponding to special cases of our model, allowing us to reduce the parametric dimension of our model from 13 to 5 parameters. Interestingly, we observe in the reduced model a phenomenon of meta-stability [30, 28], also called quasi-stability, in which the seemingly stable state reached after 30 hours following the initiation of the experiment, is followed after 300 hours by a reversed stable state. On the time scale of the experiments, we show that certain changes in the environment, like an elevation of skin surface pH, create favorable conditions for the emergence and colonization of the skin by the opportunistic pathogen population. Such predictions can help identify potential therapeutic strategies for the treatment of skin conditions involving microbiome dysbiosis, and underscore the importance of meta-stable states in the real biological processes at their different time scales.

2 Initial ODE model with 13 parameters

The model built in this paper considers two types of bacterial populations. The first population, S_c, regroups commensal bacteria species having an overall beneficial effect for the skin, and the second population, S_p, represents opportunistic pathogens. The differential equations for both bacterial populations are based on the common logistic growth model [32], considering non-explicitly the limitations in food and space. The limited resources are included in the parameters K_{sc} and K_{sp}, representing the optimum concentration of the populations in a given environment, considering the available resources.

The bactericidal effect of antimicrobial peptides (AMPs) produced by skin cells, Amp_h, on S_p is included with a Hill function. This type of highly non-linear functions have been used previously to model the effect of antibiotics on bacterial populations [22]. For the sake of simplicity, the AMPs produced by skin cells is introduced as a constant parameter, $[Amp_h]$, in the model. It represents the average concentration of these AMPs among surface cells, under given human genetic background and environmental conditions.

Several studies revealed that commensal bacterial populations, like *S. epidermidis* or *S. hominis*, are also able to produce AMPs targeted against opportunistic pathogens, such as *S. aureus* [6, 23]. For these reasons, we introduce in the model AMPs of bacterial origin, Amp_b, acting similarly to Amp_h on the pathogenic population S_p. Amp_b is produced at rate k_c by S_c, and degraded at rate d_a. Furthermore, we include a defense mechanism of S_p against S_c with a direct killing effect.

Altogether, this gives us the following ODE system with 3 variables and 13 parameters, all taking non-negative values:

$$
\begin{cases}
\dfrac{d[S_c]}{dt} = \left(r_{sc}\left(1 - \dfrac{[S_c]}{K_{sc}}\right) - \dfrac{d_{sc}[S_p]}{C_1 + [S_p]} \right)[S_c] \\[4mm]
\dfrac{d[S_p]}{dt} = \left(r_{sp}\left(1 - \dfrac{[S_p]}{K_{sp}}\right) - \dfrac{d_{spb}[Amp_b]}{C_{ab} + [Amp_b]} - \dfrac{d_{sph}[Amp_h]}{C_{ah} + [Amp_h]} \right)[S_p] \\[4mm]
\dfrac{d[Amp_b]}{dt} = k_c[S_c] - d_a
\end{cases}
\tag{1}
$$

The model is illustrated on Fig. 1 and Table 1 recapitulates the variables and the parameters with their unit.

Such a model cannot be solved analytically. Furthermore, the use of optimization algorithms to infer the 13 parameter values from data resulted in many valid sets of parameter values. Therefore, it is clearly necessary to restrict the number of parameters by identifying some of them, to be able to analyze the model.

Table 1. List of the parameters and variables of our mathematical model with their units. CFU = Colony forming unit, AU = Arbitrary Unit, ASU = Arbitrary Surface Unit

Variable	Interpretation (unit)
$[S_c]$	Surface apparent concentration of S_c ($CFU.ASU^{-1}$)
$[S_p]$	Surface apparent concentration of S_p ($CFU.ASU^{-1}$)
$[Amp_b]$	Concentration of Amp_b ($AU.ASU^{-1}$)
Parameter	**Interpretation (unit)**
r_{sc}	Growth rate of S_c (h^{-1})
r_{sp}	Growth rate of S_p, (h^{-1})
K_{sc}	Optimum concentration of S_c ($CFU.ASU^{-1}$)
K_{sp}	Optimum concentration of S_p ($CFU.ASU^{-1}$)
d_{sc}	Maximal killing rate of S_c by S_p (h^{-1})
C_1	Concentration of S_p inducing half the maximum killing rate d_{sc} ($CFU.ASU^{-1}$)
d_{spb}	Maximal killing rate of S_p by Amp_b, (h^{-1})
C_{ab}	Concentration of Amp_b inducing half the maximum killing rate d_{spb} ($AU.ASU^{-1}$)
d_{sph}	Maximal killing rate of S_p by Amp_h, (h^{-1})
C_{ah}	Concentration of Amp_h inducing half the maximum killing rate d_{sph} ($AU.ASU^{-1}$)
$[Amp_h]$	Concentration of AMPs produced by the skin cells ($AU.ASU^{-1}$)
k_c	Production rate of Amp_b by S_c ($AU.h^{-1}.CFU^{-1}$)
d_a	Degradation rate of Amp_b ($AU.h^{-1}$)

3   Using published experimental data to define relations between model parameters by steady-state reasoning

The amount of quantitative experimental data available for the model calibration is very limited due to the difficulty of carrying out experiments involving co-cultures of different bacterial species. Most of the published work focuses on single species or on measuring the relative abundances of species living on the skin, which is highly variable between individuals and skin sites [10]. In the case of AD specifically, *S. aureus* is considered pathogenic and *S. epidermidis* commensal. Published data exist however for those species which we can use to constrain the parameter values of the model.

Two series of *in vitro* experiments are considered [23, 14]. While *in vitro* cultures, even on epidermal equivalent, do not entirely capture the native growth
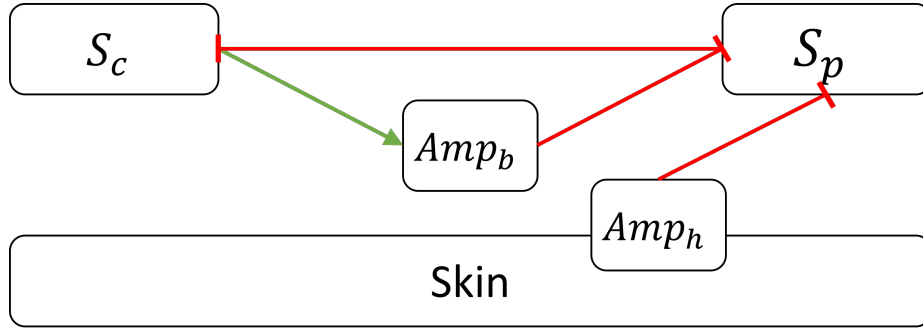
Fig. 1. Model overview, green arrow representing production and red T-lines representing killing effect.

of bacteria on human skin, they provide useful quantitative data that would be very difficult to measure *in vivo*.

In the first experiment [14], mono-cultures and co-cultures of *S. epidermidis* and *S. aureus* were allowed to develop on a 3D epidermal equivalent. Table 2 recapitulates the population sizes of the two species measured after 48 hours of incubation. Kohda *et al.* also performed another co-culture experiment where *S.epidermidis* was inoculated 4 hours prior to *S.aureus* in the media. This data is not used here as it requires additional manipulation to match the situation represented by the model. However, it would be interesting to use it in the future for model validation.

In the second experiment [23] the impact of human (LL-37) and bacterial (*Sh*-lantibiotics) AMPs on *S. aureus* survival was studied. The experiments were performed *in vitro*, and the *S. aureus* population size was measured after 24 hours of incubation. Table 3 summarizes their observations.

Table 2. Experimental data from Kohda et. al [14] used for identifying parameter values.

	S. epidermidis (CFU/well)	*S. aureus* (CFU/well)
Mono-cultures	4.10^8	3.10^9
Co-cultures	1.10^8	1.10^9

3.1   Parameter values inferred from mono-culture experiment data

We consider first the monocultures experiments from Kohda *et al.* [14], representing the simplest experimental conditions. *S. epidermis* is a representative of

Table 3. Experimental data from Nakatsuji et. al [23] used for identifying parameter relations.

Sh-lantibiotics (μM)	LL-37 (μM)	*S. aureus* (CFU/mL)
0	4	10^9
0	8	6.10^5
0.32	0	5.10^8
0.64	0	3.10^3

the commensal population S_c, and *S. aureus* of the pathogenic one, S_p. Since the two species are not interacting, the set of equations simplifies to:

$$\begin{cases} \dfrac{d[S_c]}{dt} = \left(r_{sc}\left(1 - \dfrac{[S_c]}{K_{sc}}\right)\right)[S_c] \\[4mm] \dfrac{d[S_p]}{dt} = \left(r_{sp}\left(1 - \dfrac{[S_p]}{K_{sp}}\right)\right)[S_p] \end{cases} \qquad (2)$$

At steady-state, the population concentrations are either zero, or equal to their optimum capacities (K_{sc} or K_{sp}) when the initial population concentration is non-zero. Given the rapid growth of bacterial population, the experimental measurements done after 48 hours of incubation can be considered as corresponding to a steady-state, which gives:

$$K_{sc} = 4.10^8 \; CFU.ASU^{-1} \qquad (3)$$

$$K_{sp} = 3.10^9 \; CFU.ASU^{-1} \qquad (4)$$

3.2   Parameter relations inferred from experimental data on AMP

The experimental conditions of Nakatsuji *et al.* [23] correspond to the special case where there is no commensal bacteria alive in the environment, only the bacterial AMPs, in addition to those produced by the skin cells. Our system of equations then reduces to:

$$\frac{d[S_p]}{dt} = \left(r_{sp}\left(1 - \frac{[S_p]}{K_{sp}}\right) - \frac{d_{spb}[Amp_b]}{C_{ab} + [Amp_b]} - \frac{d_{sph}[Amp_h]}{C_{ah} + [Amp_h]}\right)[S_p] \qquad (5)$$

The concentrations in LL-37 and *Sh*-lantibiotics, translated in our model into $[Amp_h]$ and $[Amp_b]$ respectively, are part of the experimental settings. Therefore, we consider them as constants over time. At steady state, we get:

$$[S_p]^* = 0 \quad \text{or} \quad [S_p]^* = K_{sp}\left(1 - \frac{d_{spb}[Amp_b]}{r_{sp}(C_{ab} + [Amp_b])} - \frac{d_{sph}[Amp_h]}{r_{sp}(C_{ah} + [Amp_h])}\right)$$

(6)

Let us first focus on the special case where no Sh-lantibiotics were introduced in the media, translating into $[Amp_b] = 0$ in our model. We consider again that the biological observations after 24 hours of incubation correspond to steady-state and substitute the experimental values measured
$[Amp_h] = 4\,\mu M$; $[S_p]^* = 10^9$ CFU, and $[Amp_h] = 8\,\mu M$; $[S_p]^* = 6.10^5$ CFU, together with the values of K_{sc} and K_{sp} (from (3) and (4)) in (6), to obtain the following equations:

$$\begin{cases} \dfrac{d_{sph}}{r_{sp}} = \dfrac{4 + C_{ah}}{6} \\[4mm] \dfrac{d_{sph}}{r_{sp}} = \dfrac{(10^4 - 2)(C_{ah} + 8)}{8.10^4} \end{cases}$$

(7)

which reduce to $C_{ah} = 8$ and $\frac{d_{sph}}{r_{sp}} = 2$.

Following the same method with the experimental conditions without any LL-37 (i.e. $[Amp_h] = 0$) and using two data points
($[Amp_b] = 0.32\,\mu M$; $[S_p]^* = 5.10^8$ CFU) and ($[Amp_b] = 0.64\,\mu M$; $[S_p]^* = 3.10^3$ CFU),
we get $C_{ab} = 0.16$ and $\frac{d_{spb}}{r_{sp}} = \frac{5}{4}$.

It is notable that the maximum killing rates of S_p by Amp_b and Amp_h are both proportional to S_p growth rate. Interestingly, such proportional relation has been observed experimentally between the killing rate of *Escherichia coli* by an antibiotic and the bacterial growth rate [31].

To be consistent with the ranges of Sh-lantibiotics concentrations described in Nakatsuji *et al.* [23], $[Amp_b]$ should take positive values below 10. Given that $[Amp_b]^* = \frac{k_c[S_c]^*}{d_a}$ at steady-state, and that $K_{sc} = 4.10^8$ CFU is the upper bound for $[S_c]^*$, we obtain the following constraint:

$$\frac{k_c}{d_a} \leq \frac{1}{4.10^7}$$

(8)

3.3   Parameter relations inferred from co-culture data

The initial model described earlier is representative of the experimental settings of the co-culture conditions described in Kohda *et al.* [14]. At steady-state, the system (1) gives:

$$[S_c]^* = 0 \quad \text{or} \quad [S_c]^* = K_{sc}\left(1 - \frac{d_{sc}[S_p]^*}{r_{sc}(C_1 + [S_p]^*)}\right)$$

(9)

$$[S_p]^* = 0 \quad \text{or} \quad [S_p]^* = K_{sp} \left(1 - \frac{d_{spb}[Amp_b]}{r_{sp}(C_{ab} + [Amp_b])} - \frac{d_{sph}[Amp_h]}{r_{sp}(C_{ah} + [Amp_h])} \right) \tag{10}$$

$$[Amp_b]^* = \frac{k_c[S_c]^*}{d_a} \tag{11}$$

Considering that what is observed experimentally after 48 hours of incubation is at steady-state, one can replace $[S_c]^*$ and $[S_p]^*$ with the experimental data point ($S.\ epidermidis = 10^8$ CFU; $S.\ aureus = 10^9$ CFU) in (9) and (10) to get the following parameter relation:

$$\frac{d_{sc}}{r_{sc}} = \frac{3}{4.10^9}C_1 + \frac{3}{4} \tag{12}$$

$$\frac{2}{3}r_{sp} = \frac{d_{sph}[Amp_h]}{C_{ah} + [Amp_h]} + \frac{10^8 d_{spb}k_c}{d_a C_{ab} + 10^8 k_c} \tag{13}$$

By integrating the values found for C_{ah} and C_{ab}, and the relations involving d_{sph} and d_{spb} into (13), we end up with:

$$d_a = 10^8 k_c \frac{56 + 31[Amp_h]}{2.56\,(4 - [Amp_h])} \quad \text{with } [Amp_h] < 4 \tag{14}$$

4   Reduced model with 5 parameters

Using the previously mentioned experimental data, and assuming they represent steady state conditions of the initial model (1), we have reduced the parametric dimension of the model from 13 to 5. Specifically, out of the original 13 parameters, we could define the values of 4 of them, and derive 4 functional dependencies from the values of the remaining parameters, as summarized in Table 4).

In our skin microbiome model (1), the parameters that remain unknown are thus:

- r_{sc}, the growth rate of S_c which can reasonably take values between 0 and 2 h^{-1} following [7,3];
- r_{sp}, the growth rate of S_p, taking similar values in the interval between 0 and 2 h^{-1};
- C_1, the concentration of S_p that induces half the maximum killing rate d_{sc} (in $CFU.ASU^{-1}$) and is thus bounded by the optimum concentration of S_p, i.e. $K_{sp} = 3.10^9\ CFU.ASU^{-1}$, as calculated in section 3.1 from [14];
- k_c, the production rate of $[Amp_b]$ chosen to take values between 0 and 0.1 $AU.h^{-1}.CFU^{-1}$, and shown to have a limited impact on the steady-state values in section 4.2;
- $[Amp_h]$, the concentration in $AU.ASU^{-1}$ of AMPs produced by skin cells between 0 and 4 (equation (14)).

Table 4. Summary of the parameter relations embedded in the reduced model.

Parameter	Value or relation to other parameters
K_{sc}	4.10^8
K_{sp}	3.10^9
C_{ah}	8
C_{ab}	0.16
d_{sph}	$2\,r_{sp}$
d_{spb}	$\frac{5}{4}\,r_{sp}$
d_{sc}	$r_{sc}\left(\dfrac{3}{4.10^9}\,C_1 + \dfrac{3}{4}\right)$
d_a	$10^8 k_c\,\dfrac{56 + 31[Amp_h]}{2.56\,(4 - [Amp_h])}$ with $[Amp_h] < 4$

4.1 Simulations at the time scale of the experiments

In order to reproduce what was observed by Kohda et. al [14], that is a dominant pathogenic population after 50 hours which can thus be considered as dysbiosis in our skin microbiome model, it is sufficient to fix a relatively low concentration of Amp produced by the skin cells, i.e. $Amph_h = 1.5$, and some fixed values for the four other parameters chosen in their intervals described above. Among a continuum of possible solutions, we chose $r_{sc} = 0.5$, $r_{sp} = 1$, $C_1 = 5.10^6$, $k_c = 0.01$.

The doses of *S. epidermidis* and *S. aureus* applied at the surface of the 3D epidermal equivalent at the beginning of the experiment ($10^5 CFU/mL$ and $10^3 CFU/mL$ respectively) are used as the initial concentrations for $[S_c]$ and $[S_p]$ respectively. Fig. 2 shows the result of a numerical simulation[3] of our model with those parameters which are in accordance to the co-culture experiments of Kohda et. al and reproduce a consistent qualitative behavior [14].

Our model can also be used to reproduce what is considered a balanced microbiome, corresponding to the commensal population being significantly more abundant than the pathogenic one. This requires modifying some parameter values to represent a less virulent pathogenic population, closer to the physiological context, given that the experiments from Kohda et. al [14] were performed using a virulent methicillin-resistant *S. aureus* strain.

We chose $r_{sp} = 0.5$, $C_1 = 2.10^8$ and a higher production of AMPs by the skin cells, $[Amp_h] = 3$, to compensate for feedback loops or stimuli that might be missing in the 3D epidermal equivalent used. Fig. 3 shows a simulation trace

---

[3] All computation results presented in this paper have been done using the BIOCHAM software with a notebook runnable online and available at https://lifeware.inria.fr/wiki/Main/Software#CMSB22b.
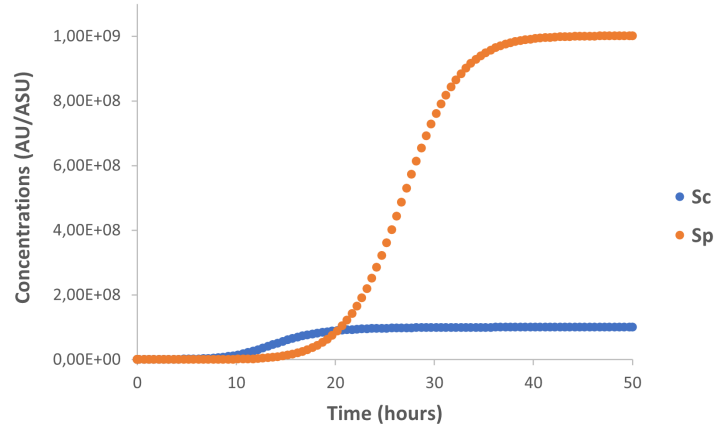
Fig. 2. Numerical simulation of the reduced ODE model over 50 hours, with initial conditions $[S_c] = 10^5$, $[S_p] = 10^3$, $[Amp_b] = 0$ and parameter values $[Amp_h] = 1.5$, $r_{sc} = 0.5$, $r_{sp} = 1$, $C_1 = 5.10^6$, $k_c = 0.01$, to fit Kohda et al. co-culture data [14] (Table 2).

obtained under those conditions which clearly indicates the dominance of the non-pathogenic population under those conditions.

4.2 Parameter sensitivity and robustness analyses

Since the previous simulations rely on some choices of values for the unknown parameters, it is important to evaluate the robustness of the predictions of our model by performing an analysis of sensitivity to the parameter values. This is possible in Biocham by specifying the property of interest in quantitative temporal logic [29]. The interesting property here is the stabilization at the time scale of the experiments around 48 hours of the bacterial population sizes to the values given by simulation (Fig. 3), Here we use the temporal logic formula:
$F(Time == 40 \wedge NSc = x1 \wedge NSp = y1 \wedge F(G(NSc = x2 \wedge NSp = y2)))$
and objective values equal to 1 for the free variables $x1, x2, y1, y2$, to express that the normalized variables NSc and NSp, i.e. current values of Sc and Sp divided by their expected value at steady state, respectively 10^8 and 10^9 in the pathogenic case of Kohda et al. experiments, is reached (F, finally) at time around 40 and finally at the end of the time horizon (FG) of 50 hours. On a given simulation trace, the free variables of the formula have a validity domain (here fixed values) which is used to define a continuous degree of satisfaction of the property as a distance to the objective values, and a robustness degree by sampling parameter values around their nominal values [29].

The sensitivity analysis (Table 5) reveals that the dominance of the commensal population is highly sensitive to variations of the initial concentration of the pathogen. To a lesser extend, the dominant population is also sensitive to the
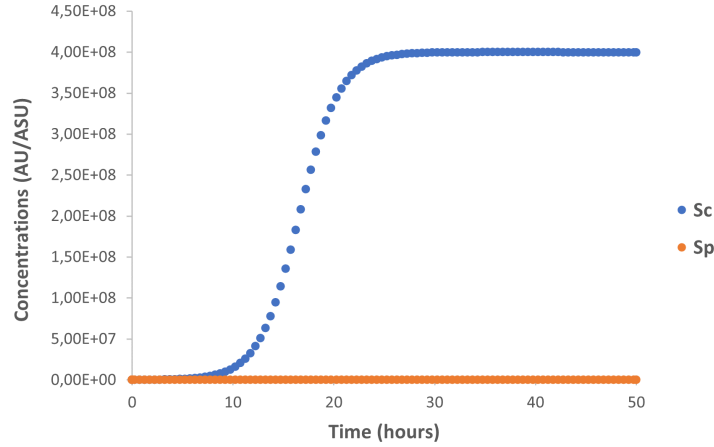
Fig. 3. Numerical simulation of the reduced ODE model over 50 hours, with initial conditions $[S_c] = 10^5$, $[S_p] = 10^3$, $[Amp_b] = 0$ and parameter values $r_{sc} = r_{sp} = 0.5$, $C_1 = 2.10^8$, $k_c = 0.01$, $[Amp_h] = 3$ corresponding to Kohda et al. experiments [14].

growth rates (r_{sc} and r_{sp}) and the concentration of human AMPs ($[Amp_h]$). On the other hand, C_1 and k_c do not seem to affect the relative proportions of the bacterial populations.

4.3   Meta-stability revealed by simulation on a long time scale

Interestingly, by extending the simulation time horizon to a longer time scale of 500 hours, one can observe a meta-stability phenomenon, shown in Fig. 4. The seemingly stable state observed in Fig. 3 at the relevant time scale of 50 hours of the experiments, is thus not a mathematical steady state, but a meta-stable state, also called quasi-stable state, that slowly evolves, with $\frac{d[S_c]}{dt} \neq 0$ and $\frac{d[S_p]}{dt} \neq 0$, towards a true stable state of the model reached around 300 hours in which the population density are reversed.

The S_c population almost reaches its optimum capacity K_{sc} after approximately 30 hours and stays relatively stable for around 100 hours more, that is over 4 days, which can reasonably be considered stable on the microbiological time scale. Meanwhile, the S_p population is kept at a low concentration compared to S_c, even though it is continuously increasing and eventually leading to its overtake of S_c.

Table 5. Sensitivity of the model to variations of the parameters and initial concentrations for the property of reaching the same values at time 40 and time horizon 50 as in Fig. 3.

Parameter	Coefficient of variation	Robustness degree
r_{sc}	0.2	0.62
r_{sp}	0.2	0.57
C_1	10	0.95
k_c	1	0.95
$[Amp_h]$	0.2	0.53
$[S_p](t=0)$	10	0.23
$[S_c](t=0)$	10	0.58
(r_{sc}, r_{sp})	0.2	0.48
$([S_c](t=0), [S_p](t=0))$	10	0.31

By varying the parameters values, it appears that this meta-stability phenomenon emerges above a threshold value of 2.5 for $[Amp_h]$ [4], that is for almost half of its possible values (see section 4).

That phenomenon of meta-stability, also called quasi-stability, is a classical notion of dynamical systems theory, particularly well-studied in the case of oscillatory systems for which analytical solutions exist, and as models of brain activity [30]. It is worth noting that it has also been considered in the computational systems biology community with respect to model reduction methods based on the identification of different regimes corresponding to different preponderant terms of the ODEs, for which simplified dynamics can be defined, and chained within a hybrid automaton [28].

More generally, this raises the question of the existence and importance of meta-stability in real biological processes, as well as the validity of the steady state assumptions made in mathematical modeling methods to fit the models to the observed experimental data.

5   Conditions favoring the pathogenic population

Whether the dysbiosis observed in AD is the cause or the result of the disease is unclear [12, 13]. Infants developing AD do not necessarily have more *S. aureus* present on their skin prior to the onset of the disease compared to the healthy group [11]. This suggests that atopic skin has some characteristics enabling the

---

[4] All computation results presented in this paper have been done using the BIOCHAM software with a notebook runnable online and available at https://lifeware.inria.fr/wiki/Main/Software#CMSB22b.
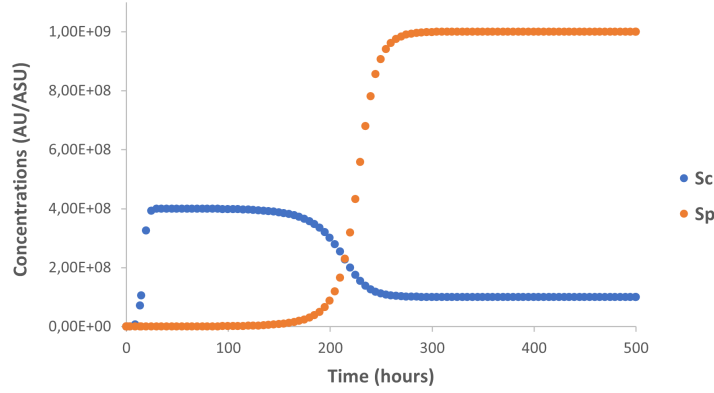
Fig. 4. Numerical simulation of the reduced ODE model on a longer time scale of 500 hours, with the same initial concentrations and parameter values as in Fig. 3, showing an inversion of the dominant bacterial population after 220 hours.

dominance of *S. aureus* over the other species of the microbiome. To test this hypothesis, we investigate two changes of the skin properties observed in AD patients (skin surface pH elevation [9] and reduced production of AMPs [25]) and their impact on the dominant species at steady-state. More specifically, we study the behavior of the system following the introduction of a pathogen and whether the pathogen will colonize the media depending on the initial concentrations of the bacterial populations and the particular skin properties mentioned before.

5.1   Skin surface pH elevation

According to Proksch [27], the physiological range for skin surface pH is 4.1-5.8. However, in certain skin conditions, like AD, an elevation of this pH has been observed. Dasgupta *et al.* studied *in vitro* the influence of pH on the growth rates of *S. aureus* and *S. epidermidis*[8]. Their experimental results show that, when the pH is increased from 5 to 6.5, the growth rate of *S. epidermidis* is multiplied by 1.8, whereas the one of *S. aureus* is multiplied by more than 4 (Table 6).

Their data can be used to select values for the growth rates r_{sc} and r_{sp} in our model, corresponding to healthy skin with a skin surface pH of 5 and compromised skin with a pH of 6.5. Because the experiments from Dasgupta *et al.* were performed *in vitro* and the bacterial population sizes measured with optical density (OD) instead of CFU, the growth rates cannot be directly translated into r_{sc} and r_{sp}. We use $r_{sc} = 0.5$ as the reference value for the commensal growth rate at pH 5, following on from previous simulation (Fig. 3). Maintaining the ratio between the two population growth rates at pH 5 and the multiplying factors following the pH elevation from Dasgupta *et al.* experimental data, we can define two sets of values for r_{sc} and r_{sp}:

Table 6. Experimental data from Dasgupta et. al [8] showing the influence of pH on growth rates of *S. epidermidis* and *S. aureus*

pH	Growth rate (ΔOD/hour)	
	S. aureus	*S. epidermidis*
5	0.03	0.05
5.5	0.04	0.07
6	0.09	0.08
6.5	0.13	0.09
7	0.14	0.10

$$\text{skin surface pH of 5} \quad \Rightarrow r_{sc} = 0.5,\ r_{sp} = 0.3$$

$$\text{skin surface pH of 6.5} \quad \Rightarrow r_{sc} = 0.9,\ r_{sp} = 1.3$$

Considering the healthy skin scenario with a skin surface pH of 5, the influence of the bacterial populations initial concentrations on the dominant species after 50 hours is evaluate using the temporal logic formula:

$$F(\text{Time} == 40 \wedge ([S_c] > u1\,[S_p]) \wedge F(G([S_c] > u2\,[S_p])))$$

where $u1$ and $u2$ are free variables representing the abundance factors between both populations, evaluated at Time= 40 and at the last time point of the trace respectively (F stands for finally and G for globally at all future time points), i.e. at the time horizon of the experiments of 50 hours.

When given with an objective value, e.g. $u1 = 10$, the distance between that value and the validity domain of the formula, i.e. the set of values for $u1$ that satisfy the formula, provides a violation degree which is used to evaluate the satisfaction degree of the property.

Here, we evaluate how much the temporal formula $F(\text{Time} == 40 \wedge ([S_c] > u1\,[S_p]) \wedge F(G([S_c] > u2\,[S_p])))$, $u1 \to 10$, $u2 \to 10$, is satisfied given variations of the initial concentrations of two populations (Fig. 5). The model predicts that, under the healthy skin condition, the commensal population will always dominate after 50 hours, except when introduced at a relatively low concentration ($< 2.10^4$) while the initial concentration of the pathogenic population is high ($> 5.10^5$).

The model predicts a higher vulnerability of the skin regarding invading pathogens with an elevated skin surface pH. When evaluating the same temporal formula with growth rates values corresponding to a skin surface pH of 6.5, we observe that even when the initial concentration of commensal is high ($> 10^7$), the pathogenic population is able to colonize the skin when introduced at a concentration as low as 3.10^4 (Fig. 6).
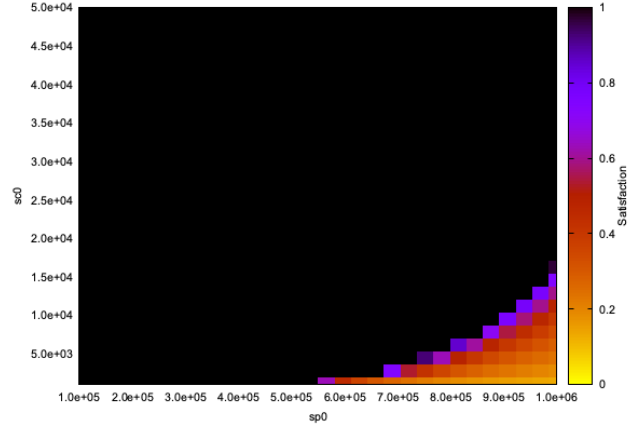
Fig. 5. Landscape of satisfaction degree of the temporal formula corresponding to healthy skin with a skin surface pH of 5 ($r_{sc} = 0.5$ and $r_{sp} = 0.3$). The x and y axis represent variations of the initial quantities of $[S_p]$ and $[S_c]$ respectively. The color coding corresponds to the satisfaction degree of the temporal logic formula. Values used for the other parameters: $C_1 = 2.10^8$, $k_c = 0.01$, $[Amp_h] = 3$.
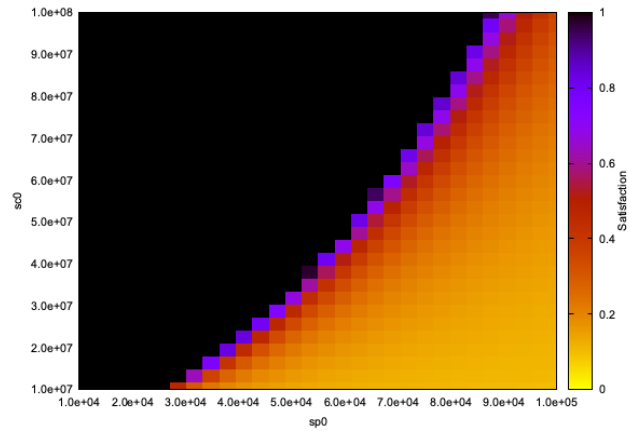

Fig. 6. Landscape of satisfaction degree of the temporal formula corresponding to compromised skin with a skin surface pH of 6.5 ($r_{sc} = 0.9$ and $r_{sp} = 1.3$). The x and y axis represent variations of the initial quantities of $[S_p]$ and $[S_c]$ respectively. The color coding corresponds to the satisfaction degree of the temporal logic formula. Values used for the other parameters: $C_1 = 2.10^8$, $k_c = 0.01$, $[Amp_h] = 3$.

Such predictions highlight the protective effect of the skin surface acidic pH against the invasion of pathogenic bacteria.

5.2   Reduced production of skin AMPs

As mentioned before, human keratinocytes constitutively produce AMPs as a defense against pathogens. In atopic dermatitis, the expression of AMPs is dysregulated, leading to lower concentration levels of AMPs in the epidermis [23]. Similarly to the analysis done for skin surface pH, our model can be used to study how the skin microbiome reacts to modulation of the AMPs production by the skin cells. Two situations are considered: an impaired production of AMPs by the skin cells ($[Amp_h] = 0.5$) and a higher concentration with $[Amp_h] = 3$. Using the same methodology as in the case of skin surface pH, the temporal logic formula $F(\text{Time} == 40 \wedge ([S_c] > u1\,[S_p]) \wedge F(G([S_c] > u2\,[S_p])))$, $u1 \rightarrow 10$, $u2 \rightarrow 10$, is evaluated for variations of the initial concentrations of both populations for $[Amp_h] = 0.5$ and $[Amp_h] = 3$ (Fig. 7).

The model predicts a slightly protective effect of Amp_h regarding the colonization of the skin by a pathogenic population, for low initial concentrations. However when both populations are introduced in high concentrations, the increase of $[Amp_h]$ appears to have the opposite effect of facilitating the colonization by the pathogenic population.

This mitigated effect might be due to the presence of $[Amp_h]$ in the constraint related to the degradation rate of $[Amp_b]$ (equation (14)) and deserves further investigation.

6   Conclusion

The objective of this research is the identification of conditions which might favor or inhibit the emergence of pathogenic populations in the skin microbiome. Such analyses can lead to insights about potential treatment strategies aiming at restoring a dysbiotic condition.

We have developed a simple ODE model of skin microbiome with 3 variables and 13 parameters which could be reduced to 5 parameters by using published data from the literature and steady state reasoning on the observations made in the biological experiments. Our bacterial population model is generic in the sense that we did not take into account the peculiarities of some specific bacterial populations, but on some general formulas of adversary population dynamics and influence factors. We showed through sensitivity analyses that our model predictions are particularly robust with respect to parameter variations.

Perhaps surprisingly, we also showed that this simple model exhibits over a large range of biologically relevant parameter values, a meta-stability phenomenon, revealed by allowing the simulation to continue for times one order of magnitude longer than the reported experimental times. This observation
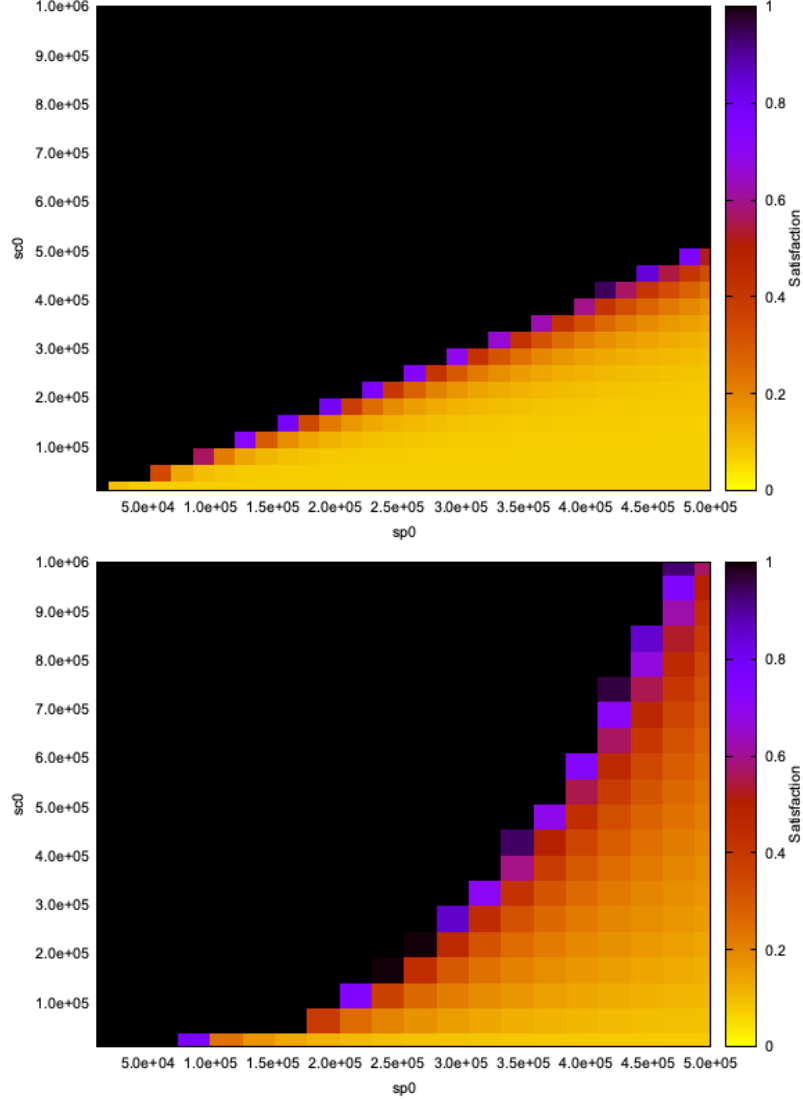
Fig. 7. Landscape of satisfaction degree of the healthy condition formula with a low concentration of human AMPs on the upper graph ($[Amp_h] = 0.5$) and a high concentration at the bottom ($[Amp_h] = 3$). The x and y axis represent variations of the initial quantities of $[S_p]$ and $[S_c]$ respectively. The color coding corresponds to the satisfaction degree of the temporal logic formula. Values used for the other parameters: $r_{sc} = r_{sp} = 0.5$, $C_1 = 2.10^8$, $k_c = 0.01$.

questions the existence and importance of meta-stability phenomena in real biological processes, whereas a natural assumption made in mathematical modeling, and model fitting to data, is that the experimental data are observed in states corresponding to real stable states of the mathematical model.

References

1. Belkaid, Y., Segre, J.A.: Dialogue between skin microbiota and immunity. Science **346**(6212), 954–959 (Nov 2014). https://doi.org/10.1126/science.1260144, https://www.science.org/doi/10.1126/science.1260144
2. Byrd, A.L., Belkaid, Y., Segre, J.A.: The human skin microbiome. Nature Reviews Microbiology **16**(3), 143–155 (Feb 2018). https://doi.org/10.1038/nrmicro.2017.157
3. Campion, J.J., McNamara, P.J., Evans, M.E.: Pharmacodynamic Modeling of Ciprofloxacin Resistance in Staphylococcus aureus. Antimicrobial Agents and Chemotherapy **49**(1), 209–219 (Jan 2005). https://doi.org/10.1128/AAC.49.1.209-219.2005, https://journals.asm.org/doi/10.1128/AAC.49.1.209-219.2005, publisher: American Society for Microbiology
4. Chopra, R., Vakharia, P.P., Sacotte, R., Silverberg, J.I.: Efficacy of bleach baths in reducing severity of atopic dermatitis: A systematic review and meta-analysis. Annals of Allergy, Asthma & Immunology **119**(5), 435–440 (Nov 2017). https://doi.org/10.1016/j.anai.2017.08.289, https://www.annallergy.org/article/S1081-1206(17)30958-4/fulltext, publisher: Elsevier
5. Cogen, A.L., Yamasaki, K., Muto, J., Sanchez, K.M., Alexander, L.C., Tanios, J., Lai, Y., Kim, J.E., Nizet, V., Gallo, R.L.: Staphylococcus epidermidis antimicrobia δ-toxin (phenol-soluble modulin-γ) cooperates with host antimicrobial peptides to kill group a streptococcus. PLOS ONE **5**(1), e8557 (Jan 2010). https://doi.org/10.1371/journal.pone.0008557, https://journals.plos.org/plosone/article?id=10.1371/journal.pone.0008557, publisher: Public Library of Science
6. Cogen, A.L., Yamasaki, K., Sanchez, K.M., Dorschner, R.A., Lai, Y., MacLeod, D.T., Torpey, J.W., Otto, M., Nizet, V., Kim, J.E., Gallo, R.L.: Selective antimicrobial action is provide by phenol-soluble modulins derived from staphylococcus epidermidis, a normal resident of the skin. Journal of Investigative Dermatology **130**(1), 192–200 (Jan 2010). https://doi.org/10.1038/jid.2009.243, https://linkinghub.elsevier.com/retrieve/pii/S0022202X15345486
7. Czock, D., Keller, F.: Mechanism-based pharmacokinetic-pharmacodynamic modeling of antimicrobial drug effects. Journal of Pharmacokinetics and Pharmacodynamics **34**(6), 727–751 (Dec 2007). https://doi.org/10.1007/s10928-007-9069-x
8. Dasgupta, A., Iyer, V., Raut, J., Qualls, A.: 16502 effect of ph on growth of skin commensals and pathogens. Journal of the American Academy of Dermatology **83**(6), AB180 (Dec 2020). https://doi.org/10.1016/j.jaad.2020.06.808, https://www.jaad.org/article/S0190-9622(20)31908-3/abstract, publisher: Elsevier

9. Eberlein-König, B., Schäfer, T., Huss-Marp, J., Darsow, U., Möhrenschlager, M., Herbert, O., Abeck, D., Krämer, U., Behrendt, H., Ring, J.: Skin surface ph, stratum corneum hydration, trans-epidermal water loss and skin roughness related to atopic eczema and skin dryness in a population of primary school children. Acta Dermato-Venereologica **80**(3), 188–191 (May 2000). https://doi.org/10.1080/000155500750042943

10. Grice, E.A., Kong, H.H., Conlan, S., Deming, C.B., Davis, J., Young, A.C., Bouffard, G.G., Blakesley, R.W., Murray, P.R., Green, E.D., Turner, M.L., Segre, J.A.: Topographical and temporal diversity of the human skin microbiome. Science (New York, N.Y.) **324**(5931), 1190–1192 (May 2009). https://doi.org/10.1126/science.1171700, https://www.ncbi.nlm.nih.gov/pmc/articles/PMC2805064/

11. Kennedy, E.A., Connolly, J., Hourihane, J.O., Fallon, P.G., McLean, W.H.I., Murray, D., Jo, J.H., Segre, J.A., Kong, H.H., Irvine, A.D.: Skin microbiome before development of atopic dermatitis: Early colonization with commensal staphylococci at 2 months is associated with a lower risk of atopic dermatitis at 1 year. J Allergy Clin. Immunol. **139**(1), 7 (2017)

12. Kobayashi, T., Glatz, M., Horiuchi, K., Kawasaki, H., Akiyama, H., Kaplan, D.H., Kong, H.H., Amagai, M., Nagao, K.: Dysbiosis and staphylococcus aureus colonization drives inflammation in atopic dermatitis. Immunity **42**(4), 756–766 (Apr 2015). https://doi.org/10.1016/j.immuni.2015.03.014, https://www.ncbi.nlm.nih.gov/pmc/articles/PMC4407815/

13. Koh, L.F., Ong, R.Y., Common, J.E.: Skin microbiome of atopic dermatitis. Allergology International p. S1323893021001404 (Nov 2021). https://doi.org/10.1016/j.alit.2021.11.001, https://linkinghub.elsevier.com/retrieve/pii/S1323893021001404

14. Kohda, K., Li, X., Soga, N., Nagura, R., Duerna, T., Nakajima, S., Nakagawa, I., Ito, M., Ikeuchi, A.: An in vitro mixed infection model with commensal and pathogenic staphylococci for the exploration of interspecific interactions and their impacts on skin physiology. Frontiers in Cellular and Infection Microbiology **11**, 712360 (Sep 2021). https://doi.org/10.3389/fcimb.2021.712360, https://www.ncbi.nlm.nih.gov/pmc/articles/PMC8481888/

15. Kong, H.H.: Skin microbiome: genomics-based insights into the diversity and role of skin microbes. Trends in Molecular Medicine **17**(6), 320–328 (Jun 2011). https://doi.org/10.1016/j.molmed.2011.01.013, https://www.sciencedirect.com/science/article/pii/S1471491411000232

16. Kong, H.H., Oh, J., Deming, C., Conlan, S., Grice, E.A., Beatson, M.A., Nomicos, E., Polley, E.C., Komarow, H.D., NISC Comparative Sequence Program, Murray, P.R., Turner, M.L., Segre, J.A.: Temporal shifts in the skin microbiome associated with disease flares and treatment in children with atopic dermatitis. Genome Research **22**(5), 850–859 (May 2012). https://doi.org/10.1101/gr.131029.111, http://genome.cshlp.org/lookup/doi/10.1101/gr.131029.111

17. Korting, H.C., Hübner, K., Greiner, K., Hamm, G., Braun-Falco, O.: Differences in the skin surface ph and bacterial microflora due to the long-term application of synthetic detergent preparations of ph 5.5 and ph 7.0. results of a crossover trial in healthy volunteers. Acta Dermato-Venereologica **70**(5), 429–431 (1990)

18. Lai, Y., Cogen, A.L., Radek, K.A., Park, H.J., MacLeod, D.T., Leichtle, A., Ryan, A.F., Di Nardo, A., Gallo, R.L.: Activation of tlr2 by a small molecule produced by staphylococcus epidermidis increases antimicrobial defense against bacterial skin infections. The Journal of investigative der-

matology **130**(9), 2211–2221 (Sep 2010). https://doi.org/10.1038/jid.2010.123, https://www.ncbi.nlm.nih.gov/pmc/articles/PMC2922455/

19. Lai, Y., Di Nardo, A., Nakatsuji, T., Leichtle, A., Yang, Y., Cogen, A.L., Wu, Z.R., Hooper, L.V., Schmidt, R.R., von Aulock, S., Radek, K.A., Huang, C.M., Ryan, A.F., Gallo, R.L.: Commensal bacteria regulate toll-like receptor 3-dependent inflammation after skin injury. Nature Medicine **15**(12), 1377–1382 (Dec 2009). https://doi.org/10.1038/nm.2062

20. Leyden, J.J., McGinley, K.J., Mills, O.H., Kligman, A.M.: Propionibacterium levels in patients with and without acne vulgaris. Journal of Investigative Dermatology **65**(4), 382–384 (Oct 1975). https://doi.org/10.1111/1523-1747.ep12607634, https://www.sciencedirect.com/science/article/pii/S0022202X1544610X

21. Malthus, T.R.T.R.: An essay on the principle of population, as it affects the future improvement of society. With remarks on the speculations of Mr. Godwin, M. Condorcet and other writers. London, J. Johnson (1798), http://archive.org/details/essayonprincipl00malt

22. Meredith, H.R., Lopatkin, A.J., Anderson, D.J., You, L.: Bacterial temporal dynamics enable optimal design of antibiotic treatment. PLOS Computational Biology **11**(4), e1004201 (Apr 2015). https://doi.org/10.1371/journal.pcbi.1004201, https://journals.plos.org/ploscompbiol/article?id=10.1371/journal.pcbi.1004201, publisher: Public Library of Science

23. Nakatsuji, T., Chen, T.H., Narala, S., Chun, K.A., Two, A.M., Yun, T., Shafiq, F., Kotol, P.F., Bouslimani, A., Melnik, A.V., Latif, H., Kim, J.N., Lockhart, A., Artis, K., David, G., Taylor, P., Streib, J., Dorrestein, P.C., Grier, A., Gill, S.R., Zengler, K., Hata, T.R., Leung, D.Y.M., Gallo, R.L.: Antimicrobials from human skin commensal bacteria protect against staphylococcus aureus and are deficient in atopic dermatitis. Science translational medicine **9**(378), eaah4680 (Feb 2017). https://doi.org/10.1126/scitranslmed.aah4680, https://www.ncbi.nlm.nih.gov/pmc/articles/PMC5600545/

24. Nakatsuji, T., Hata, T.R., Tong, Y., Cheng, J.Y., Shafiq, F., Butcher, A.M., Salem, S.S., Brinton, S.L., Rudman Spergel, A.K., Johnson, K., Jepson, B., Calatroni, A., David, G., Ramirez-Gama, M., Taylor, P., Leung, D.Y.M., Gallo, R.L.: Development of a human skin commensal microbe for bacteriotherapy of atopic dermatitis and use in a phase 1 randomized clinical trial. Nature Medicine **27**(4), 700–709 (Apr 2021). https://doi.org/10.1038/s41591-021-01256-2, https://www.nature.com/articles/s41591-021-01256-2

25. Ong, P.Y., Ohtake, T., Brandt, C., Strickland, I., Boguniewicz, M., Ganz, T., Gallo, R.L., Leung, D.Y.M.: Endogenous antimicrobial peptides and skin infections in atopic dermatitis. The New England Journal of Medicine **347**(15), 1151–1160 (Oct 2002). https://doi.org/10.1056/NEJMoa021481

26. Pazgier, M., Hoover, D.M., Yang, D., Lu, W., Lubkowski, J.: Human β-defensins. Cellular and Molecular Life Sciences CMLS **63**(11), 1294–1313 (Jun 2006). https://doi.org/10.1007/s00018-005-5540-2, http://link.springer.com/10.1007/s00018-005-5540-2

27. Proksch, E.: pH in nature, humans and skin. The Journal of Dermatology **45**(9), 1044–1052 (2018). https://doi.org/https://doi.org/10.1111/1346-8138.14489, https://onlinelibrary.wiley.com/doi/abs/10.1111/1346-8138.14489

28. Radulescu, O., Samal, S.S., Naldi, A., Grigoriev, D., Weber, A.: Symbolic dynamics of biochemical pathways as finite states machines. In: Roux, O.F., Bourdon, J. (eds.) Computational Methods in Systems Biology - 13th International Conference, CMSB 2015, Nantes, France, September 16-18, 2015, Proceedings.

Lecture Notes in Computer Science, vol. 9308, pp. 104–120. Springer (2015). https://doi.org/10.1007/978-3-319-23401-4_10

29. Rizk, A., Batt, G., Fages, F., Soliman, S.: Continuous valuations of temporal logic specifications with applications to parameter optimization and robustness measures. Theoretical Computer Science **412**(26), 2827–2839 (2011). https://doi.org/10.1016/j.tcs.2010.05.008

30. Tognoli, E., Kelso, J.A.S.: The metastable brain. Neuron **81**(1), 35–48 (01 2014). https://doi.org/10.1016/j.neuron.2013.12.022, https://pubmed.ncbi.nlm.nih.gov/24411730

31. Tuomanen, E., Cozens, R., Tosch, W., Zak, O., Tomasz, A.: The rate of killing of Escherichia coli by beta-lactam antibiotics is strictly proportional to the rate of bacterial growth. Journal of General Microbiology **132**(5), 1297–1304 (May 1986). https://doi.org/10.1099/00221287-132-5-1297

32. Zwietering, M.H., Jongenburger, I., Rombouts, F.M., van 't Riet, K.: Modeling of the bacterial growth curve. Applied and Environmental Microbiology **56**(6), 1875–1881 (Jun 1990), https://www.ncbi.nlm.nih.gov/pmc/articles/PMC184525/